International Journal of Heat and Mass Transfer 51 (2008) 5679–5686

Contents lists available at ScienceDirect

International Journal of Heat and Mass Transfer

journal homepage: www.elsevier.com/locate/ijhmt

Freezing of blood perfused tissue: An improved quasi-steady solution

Latif M. Jiji *, Peter Ganatos

Department of Mechanical Engineering, The City College of the City University of New York, New York 10031, United States

ARTICLE INFO

Article history:
Received 26 July 2007
Received in revised form 4 April 2008
Available online 12 June 2008

Keywords:
Tissue freezing
Phase change
Improved quasi-steady
Moving boundary

ABSTRACT

An approximate analytic solution is obtained for the temperature distribution and freezing front propagation in tissue. The solution accounts for blood perfusion and metabolic heat generation. The method of solution is based on the introduction of assumed temperature profiles in the frozen and unfrozen regions. The assumed profiles satisfy all boundary conditions as well as the governing heat equations at the moving interface. In addition, the steady state interface location is identically satisfied. Two cases are considered: freezing of a semi-infinite blood perfused tissue over a planar probe and around a spherical probe. The accuracy of the solution is verified in two test cases with known exact solutions: the limiting case of Neumann's problem and a numerical solution to tissue freezing around a spherical probe. The present theory represents a significant improvement over the quasi-steady model.

1. Introduction

A key factor in cryogenics and cryosurgery is predicting the propagation of the frozen front. This is critical in the application of cryosurgical probes to selectively destroy diseased tissue. Tissue freezing falls in a general class of problems variously known as phase change, moving boundary and free boundary problems. Examples of such problems are found in casting, energy storage, nuclear waste disposal, food processing and cryopreservation. The wide range of applications of phase change problems has generated a large number of publications. The most recent comprehensive bibliography lists 5869 references on melting and freezing published during the past century and a half [1]. Yet there are very few exact solutions [2–5]. The mathematical difficulty is traced to the inherent non-linearity of phase change problems. Tissue freezing is characterized by three factors: (1) blood perfusion, (2) vascular architecture and (3) metabolic heat production. Blood perfusion and metabolic heat cease in frozen tissue but remain active in the unfrozen phase. The complex nature of heat transfer in living organs and biological tissue precludes exact analytical solutions. Assumptions and simplifications must be made to make the problem tractable while capturing the essential features of the process. Not surprisingly numerical techniques are extensively used in solving tissue freezing problems [6–14].

An important consideration in the analysis of tissue freezing is the formulation of an appropriate bioheat equation. One of the earliest equations was developed and applied by Pennes in 1948 [15]. Although it does not take into consideration the vascular architecture, it does account for blood perfusion and metabolic heat generation. Because of its simplicity and reasonable accuracy under certain conditions, it has been extensively applied in heat transfer analysis of biological tissue under thawing and freezing conditions.

There is a need for simple analytic solutions to examine the effect of important parameters on tissue freezing in general and progression of the frozen front in particular. A common simplification which is extensively used in solving a variety of phase changing problems is based on the quasi-steady approximation [16–20]. In this model, the transient term in the heat equation can be neglected under certain conditions. This vastly simplifies phase changing problems and often eliminates the need for numerical solutions. Justification for neglecting the transient terms is based on the magnitude of the Stefan number which is the ratio of sensible to latent heat of fusion. The quasi-steady approximation gives exact results for the limiting case of zero sensible heat corresponding to zero Stefan number. This presents a severe limitation on the accuracy of solutions to cryosurgery problems which usually involve large temperature drops in the frozen phase leading to large sensible heat. In a recently published paper, Lin and Zheng [21] partially addressed this issue by approximately accounting for the sensible heat to improve quasi-steady solutions to freezing of a non-biological medium. This was accomplished by introducing an assumed temperature profile in the frozen region. The assumed profile makes use of Stefan's exact solution. They applied this approach to three classical one-dimensional problems involving freezing of non-biological material initially at the fusion temperature due to a sudden drop in an exposed surface temperature. The three geometries considered are a semi-infinite planar region (Stefan's problem), a cylinder and a sphere. Comparison with exact results showed excellent improvement over the quasi-steady solutions.

* Corresponding author. Tel.: +1 212 650 5228; fax: +1 212 650 8013.
E-mail addresses: jiji@ccny.cuny.edu (L.M. Jiji), ganatos@ccny.cuny.edu (P. Ganatos).

0017-9310/$ - see front matter © 2008 Elsevier Ltd. All rights reserved.
doi:10.1016/j.ijheatmasstransfer.2008.04.012

Nomenclature

c_s	specific heat of frozen tissue
c_b	specific heat of blood
k	thermal conductivity of unfrozen tissue
L	probe thickness
$\mathscr{L}$	latent heat of fusion
q_m	volumetric metabolic heat production rate
r	spherical coordinate
r_o	radius of spherical probe
St	Stefan number, defined in (3)
t	time
T	unfrozen tissue temperature
T_{a0}	arterial blood supply temperature
T_f	fusion temperature
T_i	initial temperature
T_o	surface temperature
w_b	volumetric blood perfusion rate per unit tissue volume
x	Cartesian coordinate

Subscripts

b	blood
i	interface, initial temperature
s	solid phase

Superscripts

m	coordinates designation: 0 cartesian. 2 spherical
n	exponent in the assumed unfrozen tissue temperature

Greek symbols

α	thermal diffusivity of unfrozen tissue
β	blood perfusion parameter, defined in (3)
γ	metabolic heat production parameter, defined in (3)
κ	conductivity-temperature ratio parameter, defined in (11)
θ	dimensionless temperature of tissue, defined in (3)
ρ_b	blood density
τ	dimensionless time, defined in(3)
ξ	dimensionless distance, defined in(3)
$\xi_i(\infty)$	dimensionless steady state interface position

In this paper we consider one-dimensional freezing of a blood-perfused tissue. Two geometries are considered: (1) Freezing over a planar probe and (2) freezing around a spherical probe. The Pennes bioheat equation is used to account for blood perfusion and metabolic heat generation. Although the method of Lin and Zheng cannot be applied to this problem, a new approach is introduced to improve the accuracy of the quasi-steady approximation in both the frozen and unfrozen regions. Solutions to the temperature distribution and interface motion take into consideration blood perfusion, metabolic heat generation, thermal diffusivity and Stefan number effects.

2. Analysis

2.1. Problem statement and formulation

We consider one-dimensional freezing of tissue over a planar or spherical cryosurgical probe. Fig. 1 shows a planar probe of thickness L which is maintained at temperature $T_o < T_f$. The probe is suddenly applied to a semi-infinite tissue at uniform temperature T_i which is above the freezing temperature T_f. Metabolic heat is generated throughout the tissue at a constant volumetric rate q_m in the unfrozen phase. Blood at arterial temperature T_{a0} is supplied to the unfrozen tissue at a uniform volumetric rate per unit tissue volume, w_b. A frozen front forms instantaneously at $x = 0$. Fig. 2 shows the same problem using a spherical probe of radius r_o.

2.2. Governing equations

We assume constant properties in each phase. Since metabolic activity ceases once the tissue is frozen, the governing equation in this layer is given by the classical heat equation. For the unfrozen tissue we use the Pennes bioheat equation [15]. The dimensionless forms of these equations are given by

$$\frac{1}{\xi^m}\frac{\partial}{\partial\xi}\left[\xi^m\frac{\partial\theta_s}{\partial\xi}\right]=St\frac{\partial\theta_s}{\partial\tau} \tag{1}$$

and

$$\frac{1}{\xi^m}\frac{\partial}{\partial\xi}\left[\xi^m\frac{\partial\theta}{\partial\xi}\right]-\beta\theta-\gamma=St\frac{\alpha_s}{\alpha}\frac{\partial\theta}{\partial\tau}, \tag{2}$$

where $m = 0$ is for Cartesian coordinates (planar probe) and $m = 2$ is for spherical coordinates (spherical probe). Subscript s refers to the solid phase (frozen tissue), α is thermal diffusivity and St is the *Stefan number*. The dimensionless variables and parameters in the Cartesian system are defined as

$$\theta_s=\frac{T_s-T_o}{T_f-T_o},\quad \theta=\frac{T-T_{a0}}{T_f-T_{a0}},\quad \xi=\frac{x}{L},\quad \tau=St\frac{\alpha_s}{L^2}t,$$
$$\beta=\frac{\rho_b c_b w_b L^2}{k},\quad \gamma=\frac{q_m L^2}{k(T_{a0}-T_f)},\quad St=\frac{c_s(T_f-T_o)}{\mathscr{L}}. \tag{3}$$

Subscript b refers to blood, c is specific heat and $\mathscr{L}$ is the latent heat of fusion. For spherical coordinates x is replaced by r and L by r_o.

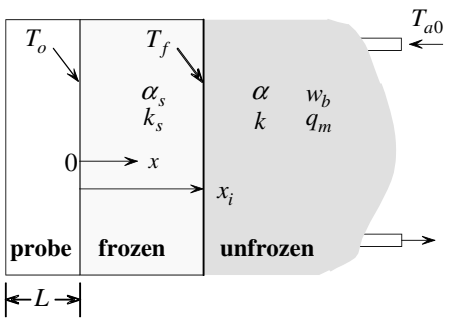

Fig. 1. Planar probe.

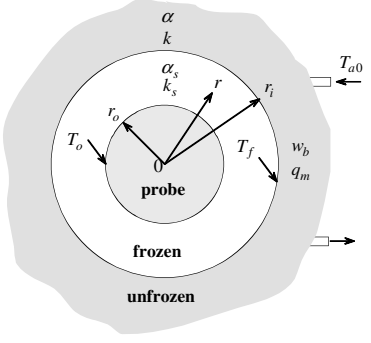

Fig. 2. Spherical probe.

2.3. Boundary and initial conditions

The dimensionless form of the boundary and initial conditions are

$$\theta_s(0,\tau) = 0 \text{ (Cartesian)}, \tag{4a}$$
$$\theta_s(1,\tau) = 0 \text{ (spherical)}, \tag{4b}$$

$$\theta_s(\xi_i,\tau) = 1, \tag{5}$$
$$\theta(\xi_i,\tau) = 1, \tag{6}$$
$$\theta(\infty,\tau) = -\gamma/\beta. \tag{7}$$

The initial conditions are

$$\theta(\xi,0) = -\gamma/\beta, \tag{8}$$

$$\xi_i(0) = 0 \text{ (Cartesian)}, \tag{9a}$$
$$\xi_i(0) = 1 \text{ (spherical)}. \tag{9b}$$

Conservation of energy at the interface gives

$$\frac{d\xi_i}{d\tau} = \frac{\partial\theta_s(\xi_i,\tau)}{\partial\xi} + \kappa\frac{\partial\theta(\xi_i,\tau)}{\partial\xi}, \tag{10}$$

where κ is defined as

$$\kappa = \frac{k(T_{a0}-T_f)}{k_s(T_f-T_o)}. \tag{11}$$

Examination of the dimensionless equations shows that the problem is governed by five parameters: diffusivity ratio α_s/α, blood perfusion β, metabolic heat productionγ, conductivity-temperature ratio κ, and the Stefan number *St*.

2.4. Simplified model: quasi-steady approximation

An exact analytic solution to this mathematical problem is not available. Approximate solutions to phase changing problems have been obtained based on the quasi-steady model in which the transient term in the governing equations is dropped. Quasi-steady solutions are valid for Stefan numbers that are small compared to unity. A small Stefan number corresponds to small sensible heat compared to latent heat. Thus neglecting sensible heat leads to overestimating interface location. Furthermore, quasi-steady solutions do not account for the effects of Stefan number and thermal diffusivity parameter α_s/α.

Eliminating the transient term in (1) and (2)and integrating the resulting equations gives the solution to the planar and spherical probes described in [16]. Of interest here is the solution to the transient interface location $\xi_i(\tau)$. For the planar probe it is given by

$$\tau = -\frac{\beta}{\kappa^2(\beta+\gamma)^2}\left\{\kappa\frac{\beta+\gamma}{\sqrt{\beta}}\xi_i + \ln\left|1-\kappa\frac{\beta+\gamma}{\sqrt{\beta}}\xi_i\right|\right\}. \tag{12}$$

For the spherical probe the solution is

$$\begin{aligned}\tau = &-\frac{1}{c}(\xi_i-1) + \frac{1}{2c^2}(b+c)\ln\frac{a+b\xi_i+c\xi_i^2}{a+b+c}\\ &-\frac{1}{2c\sqrt{b^2-4ac}}\left[\frac{1}{c}(b^2-2ac)+b\right]\\ &\times\ln\left[\frac{2c+b+\sqrt{b^2-4ac}}{2c+b-\sqrt{b^2-4ac}}\,\frac{2c\xi_i+b-\sqrt{b^2-4ac}}{2c\xi_i+b+\sqrt{b^2-4ac}}\right],\end{aligned} \tag{13}$$

where

$$a = -1-\kappa\frac{\beta+\gamma}{\beta},\quad b = \kappa\frac{\beta+\gamma}{\beta}(1-\sqrt{\beta}),\quad c = \kappa\frac{\beta+\gamma}{\sqrt{\beta}}. \tag{14}$$

We note that the interface solution to the planar probe depends on a single parameter $k(\beta+\gamma)/\sqrt{\beta}$. However, the solution to the spherical probe depends on an additional parameter $\sqrt{\beta}$.

2.5. Improved quasi-steady solution

The inherent limitations on quasi-steady solutions of phase changing problems motivated the search for corrective measures to improve the accuracy of the quasi-steady solution to the freezing tissue problem. Since the Stefan solution does not apply to metabolic heat production in a blood perfused tissue, the method of Lin and Zheng cannot be applied to this case. A unique feature of the tissue problem is the existence of a steady state condition corresponding to $\tau\to\infty$. This is not the case with the Stefan and Neumann problems. The exact steady state tissue temperature distribution and interface location can be easily determined.

To improve the quasi-steady solution of the tissue problem, a new approach is developed that does not require the use of exact solutions to related problems. Rather than solving the quasi-steady equations, appropriate temperature profiles are assumed for the frozen and unfrozen phases. The assumed profiles satisfy all boundary conditions as well as the two transient heat Eqs. (1) and (2) and conservation of energy at the interface (10). In addition, the assumed profiles insure that the steady state interface location coincides with the exact solution. This approach is followed in solving the two tissue freezing problems described above. It should be pointed out that this method differs from the heat balance integral approach in which the assumed profiles satisfy the integral form of the heat Eqs. (1) and (2).

2.5.1. Cartesian system planar probe

2.5.1.1. Assumed temperature profiles. Since the frozen region is finite while the unfrozen phase is semi-infinite, assumed profiles take on different forms. The following polynomial profile is assumed for the frozen tissue

$$\theta_s(\xi,\tau) = a_0 + a_1\left[\frac{\xi}{\xi_i}-1\right] + a_2\left[\frac{\xi}{\xi_i}-1\right]^2. \tag{15}$$

For the semi-infinite unfrozen tissue the following exponential form is assumed

$$\theta(\xi_i,\tau) = b_0 + b_1\exp\left[-b_2\frac{\xi^n}{\xi_i^n}\right]. \tag{16}$$

The six coefficients a_0, a_1, a_2, b_0, b_1 and b_2 may be constant or functions of $\xi_i(\tau)$ and the exponent n is constant. In addition to the four boundary conditions on θ_s and θ, three additional conditions are needed. Two conditions are formulated based on the constancy of interface temperature, the satisfaction of heat Eqs. (1) and (2) at the interface, and conservation of energy (10) at the interface $\xi = \xi_i$. A third condition is based on the interface steady state solution $\xi_i = \xi_i(\infty)$. Since the temperature of the frozen region at the interface remains constant at all times, it follows that

$$d\theta_s(\xi_i,\tau) = \frac{\partial\theta_s(\xi_i,\tau)}{\partial\xi}d\xi_i + \frac{\partial\theta_s(\xi_i,\tau)}{\partial\tau}d\tau = 0.$$

Solving the above for $\frac{d\xi_i}{d\tau}$ and using (1) to eliminate $\frac{\partial\theta_s(\xi_i,\tau)}{\partial\tau}$ yields

$$\frac{d\xi_i}{d\tau} = -\frac{1}{St}\frac{\dfrac{\partial^2\theta_s(\xi_i,\tau)}{\partial\xi^2}}{\dfrac{\partial\theta_s(\xi_i,\tau)}{\partial\xi}}. \tag{17}$$

Substituting (17) into (10) gives

$$\left[\frac{\partial\theta_s(\xi_i,\tau)}{\partial\xi}\right]^2 + \kappa\frac{\partial\theta_s(\xi_i,\tau)}{\partial\xi}\frac{\partial\theta(\xi_i,\tau)}{\partial\xi} + \frac{1}{St}\frac{\partial^2\theta_s(\xi_i,\tau)}{\partial\xi^2} = 0. \tag{18}$$

Similarly, constancy of the temperature of the unfrozen region at the interface, heat Eq. (2) and interface energy Eq. (10) give

$$\frac{\partial\theta_s(\xi_i,\tau)}{\partial\xi}\frac{\partial\theta(\xi_i,\tau)}{\partial\xi}+\kappa\left[\frac{\partial\theta(\xi_i,\tau)}{\partial\xi}\right]^2+\frac{1}{St}\frac{\alpha}{\alpha_s}\left[\frac{\partial^2\theta(\xi_i,\tau)}{\partial\xi^2}-\beta-\gamma\right]=0. \tag{19}$$

Finally, at steady state the interface becomes stationary and condition (10) simplifies to

$$\frac{\partial\theta_s(\xi_i,\infty)}{\partial\xi}+\kappa\frac{\partial\theta(\xi_i,\infty)}{\partial\xi}=0. \tag{20}$$

Application of boundary conditions (4-7) gives

$$a_0=1,\quad a_2=a_1-1,\quad b_0=-\gamma/\beta,\quad b_1=\left[1+\frac{\gamma}{\beta}\right]\exp b_2.$$

The assumed profiles (15) and (16) become

$$\theta_s(\xi,\tau)=1+a_1\left[\frac{\xi}{\xi_i}-1\right]+(a_1-1)\left[\frac{\xi}{\xi_i}-1\right]^2. \tag{21}$$

and

$$\theta(\xi,\tau)=-\frac{\gamma}{\beta}+\frac{\gamma+\beta}{\beta}\exp\left[b_2-b_2\frac{\xi^n}{\xi_i^n}\right]. \tag{22}$$

Application of (21) and (22) to conditions (18)–(20) gives three equations for a_1, b_2 and n:

$$a_1^2-\kappa\left[1+\frac{\gamma}{\beta}\right]na_1b_2+\frac{1}{St}(a_1-1)=0, \tag{23}$$

$$-na_1+\kappa\left[1+\frac{\gamma}{\beta}\right]n^2b_2-\frac{1}{St}\frac{\alpha}{\alpha_s}\left[n^2(1-b_2)-n+\frac{\beta\xi_i^2}{b_2}\right]=0, \tag{24}$$

and

$$n=\frac{a_1(\infty)}{\kappa[1+(\gamma/\beta)]b_2(\infty)}. \tag{25}$$

Evaluating (23) and (24) at $\tau=\infty$ and combining the resulting equations with (25) gives three equations for $a_1(\infty)$, $b_2(\infty)$ and n. The solution to the three equations gives the constant n

$$n=1+\frac{1}{\kappa[1+(\gamma/\beta)]}-\beta\kappa[1+(\gamma/\beta)]\xi_i^2(\infty). \tag{26}$$

The exact solution to the steady state interface location $\xi_i(\infty)$is easily determined and will not be detailed here. Setting the transient terms in (1) and (2) equal to zero, solving the resulting equations, satisfying boundary conditions Eqs. (4)–(7) and substituting into interface condition (2) gives

$$\xi_i(\infty)=\frac{1}{\kappa[1+(\gamma/\beta)]\sqrt{\beta}}. \tag{27}$$

Substituting (27) into (26) gives

$$n=1. \tag{28}$$

With n determined, MATLAB is used to solve (23) and (24) for a_1 and b_2 as functions of ξ_i.

2.5.1.2. Interface motion. To determine the interface location, (21) and (22) are substituted into (10)

$$\frac{d\xi_i}{d\tau}=\frac{a_1}{\xi_i}-\kappa\left[1+\frac{\gamma}{\beta}\right]\frac{b_2}{\xi_i}. \tag{29}$$

Solutions to a_1 and b_2 are substituted into (29) and the resulting equation is integrated numerically using initial condition (9a) to give the transient solution to the interface location.

2.5.2. Spherical system: spherical probe

The procedure leading to conditions (18) and (19) is repeated using heat Eqs. (1) and (2) in spherical coordinates ($m=2$). Thus (18) and (19) are replaced by

$$\left[\frac{\partial\theta_s(\xi_i,\tau)}{\partial\xi}\right]^2+\kappa\frac{\partial\theta_s(\xi_i,\tau)}{\partial\xi}\frac{\partial\theta(\xi_i,\tau)}{\partial\xi}+\frac{1}{St}\left[\frac{\partial^2\theta_s(\xi_i,\tau)}{\partial\xi^2}+\frac{2}{\xi}\frac{\partial\theta_s(\xi_i,\tau)}{\partial\xi}\right]=0, \tag{30}$$

$$\frac{\partial\theta_s(\xi_i,\tau)}{\partial\xi}\frac{\partial\theta(\xi_i,\tau)}{\partial\xi}+\kappa\left[\frac{\partial\theta(\xi_i,\tau)}{\partial\xi}\right]^2+\frac{1}{St}\times\frac{\alpha}{\alpha_s}\left[\frac{\partial^2\theta(\xi_i,\tau)}{\partial\xi^2}+\frac{2}{\xi}\frac{\partial\theta(\xi_i,\tau)}{\partial\xi}-\beta-\gamma\right]=0. \tag{31}$$

The assumed profile in the frozen tissue takes the form

$$\theta_s(\xi,\tau)=1+a_1\left[\frac{\xi_i}{\xi}-1\right]+a_2\left[\frac{\xi_i}{\xi}-1\right]^2. \tag{32}$$

However, the temperature profile in the semi-infinite unfrozen tissue, (16), is assumed to apply to both Cartesian and spherical systems. Application of boundary conditions Eqs. 4–7 to (16) and (32) gives

$$a_0=1,\quad a_2=-\frac{1+a_1(\xi_i-1)}{(\xi_i-1)^2},\quad b_0=-\gamma/\beta,\quad b_1=\left[1+\frac{\gamma}{\beta}\right]\exp b_2.$$

The assumed profiles (32) and (16) become

$$\theta_s(\xi,\tau)=1+a_1\left[\frac{\xi_i}{\xi}-1\right]-\frac{1+a_1(\xi_i-1)}{(\xi_i-1)^2}\left[\frac{\xi_i}{\xi}-1\right]^2 \tag{33}$$

and

$$\theta(\xi_i,\tau)=-\frac{\gamma}{\beta}+\frac{\gamma+\beta}{\beta}\exp\left[b_2-b_2\frac{\xi^n}{\xi_i^n}\right]. \tag{34}$$

Application of (33) and (34) to conditions (30), (31) and (20) gives three equations for a_1, b_2 and n:

$$a_1^2+\kappa\left[1+\frac{\gamma}{\beta}\right]na_1b_2-\frac{2}{St}\left[\frac{a_1}{(\xi_i-1)}+\frac{1}{(\xi_i-1)^2}\right]=0, \tag{35}$$

$$na_1+\kappa\left[1+\frac{\gamma}{\beta}\right]n^2b_2-\frac{1}{St}\frac{\alpha}{\alpha_s}\left[n^2(1-b_2)+n+\frac{\beta\xi_i^2}{b_2}\right]=0 \tag{36}$$

and

$$n=\frac{-a_1(\infty)}{\kappa[1+(\gamma/\beta)]b_2(\infty)}. \tag{37}$$

Evaluating (35) and (36) at $\tau=\infty$ and combining the resulting equations with (37) gives three equations for $a_1(\infty)$, $b_2(\infty)$ and n. The solution to the three equations gives the constant n

$$n=\frac{1}{[\xi_i(\infty)-1]\kappa[1+(\gamma/\beta)]}+\beta\kappa[1+(\gamma/\beta)][1-\xi_i(\infty)]\xi_i^2(\infty)-1. \tag{38}$$

The exact solution to the steady state interface location $\xi_i(\infty)$ for the spherical probe is given by

$$\xi_i(\infty)=\frac{\sqrt{\beta}-1}{2\sqrt{\beta}}+\frac{1}{2\sqrt{\beta}}\left\{(1-\sqrt{\beta})^2+4\sqrt{\beta}\left[1+\frac{\beta}{\kappa(\beta+\gamma)}\right]\right\}^{\frac{1}{2}}. \tag{39}$$

2.5.2.1. Interface motion. Interface motion is determined by substituting (33) and (34) into (10)

$$\frac{d\xi_i}{d\tau}=-\frac{a_1}{\xi_i}-\kappa\left[1+\frac{\gamma}{\beta}\right]\frac{nb_2}{\xi_i}. \tag{40}$$

Numerical integration of (40) using initial condition (9b) gives the solution to the spherical interface motion.

3. Results and discussion

3.1. Solution accuracy

To evaluate the accuracy of the present theory, two test cases are carried out. In the first, comparison is made with the limiting case of Neumann's solution. This is the exact solution to the classical problem of planar solidification of a semi-infinite region [2]. In the second, comparison is made with a numerical solution to freezing of blood perfused tissue around a spherical cryoprobe [16].

3.1.1. Test case 1: Neumann's problem

This is a special case of the more general freezing problem of a semi-infinite tissue. The improved quasi-steady solution to this problem is obtained by setting blood perfusion parameter $\beta = 0$ and metabolic heat parameter $\gamma = 0$ in Eqs. (23) and (24) to give

$$a_1^2 - \kappa a_1 b_2 + \frac{1}{St}(a_1 - 1) = 0, \tag{41}$$

$$-a_1 + \left[\kappa + \frac{1}{St}\frac{\alpha}{\alpha_s}\right] b_2 = 0. \tag{42}$$

The solutions to (41) and (42) give a_1 and b_2 as

$$a_1 = [\kappa(\alpha_s/\alpha) + (1/St)]\left[\sqrt{1 + \frac{2}{\kappa(\alpha_s/\alpha) + (1/St)}} - 1\right] \tag{43}$$

and

$$b_2 = \frac{(\alpha_s/\alpha)a_1}{\kappa(\alpha_s/\alpha) + (1/St)}. \tag{44}$$

Substituting (43) and (44) into (29), integrating and using initial condition (9a) gives the interface location

$$\frac{\xi_i}{\sqrt{2\tau}} = \left\{\frac{1}{St}\left[\sqrt{1 + \frac{2}{\kappa(\alpha_s/\alpha) + (1/St)}} - 1\right]\right\}^{\frac{1}{2}}. \tag{45}$$

Note that in the definition of κ in (11) blood supply temperature T_{a0} is replaced by the initial temperature T_i. The exact solution to Neumann's problem is given by [2]

$$\frac{(\xi_i)_{exact}}{\sqrt{2\tau}} = \lambda\sqrt{\frac{2}{St}}, \tag{46}$$

where λ is the solution to the transcendental equation

$$\frac{\exp(-\lambda^2)}{\operatorname{erf}\lambda} - \kappa\sqrt{\frac{\alpha_s}{\alpha}}\frac{\exp(\lambda^2\alpha_s/\alpha)}{1 - \operatorname{erf}(\lambda\sqrt{\alpha_s/\alpha})} = \lambda\frac{\sqrt{\pi}}{St}. \tag{47}$$

In the simplified quasi-steady model of Neumann's problem the temperature of the unfrozen phase instantaneously drops to the fusion temperature. Thus the unfrozen phase plays no role in the interface solution, which is given by

$$\frac{(\xi_i)_{quasi\text{-}steady}}{\sqrt{2\tau}} = 1 \tag{48}$$

To examine the accuracy of the present theory for improving the quasi-steady model, the three solutions for the interface location ξ_i are plotted as a function of Stefan number in Fig. 3 for $\alpha_s/\alpha = 1$. The error for the present and quasi-steady models increases with increasing κ and St. Nevertheless, the present theory gives significant improvement over the quasi-steady solution. We examine the case of $\kappa = 0.3$ where errors are highest. Comparing the quasi-steady solution with the present theory at $\kappa = 0.3$ and $St = 0.5$, the error decreases from 21% to 4%. At $St = 1$ the corresponding errors are 36% and 5%, and at $St = 3$ the error drops from 81% to 7%. Clearly, the quasi-steady solution deteriorates rapidly with increasing Stefan number while the improved solution does not. The parameter α_s/α reflects the contribution of the unfrozen tissue to interface motion. Fig. 4 gives the interface location for $\alpha_s/\alpha = 10$. While the quasi-steady solution deteriorates significantly, with errors at $\kappa = 0.3$ of 80% and 270% for $St = 0.5$ and $St = 3$, respectively, the corresponding errors of the improved solution are 9% and 10%. The special case of $\kappa = 0$ represents Stefan's problem where the unfrozen region is initially at the fusion temperature. For this case α_s/α has no effect on the interface motion.

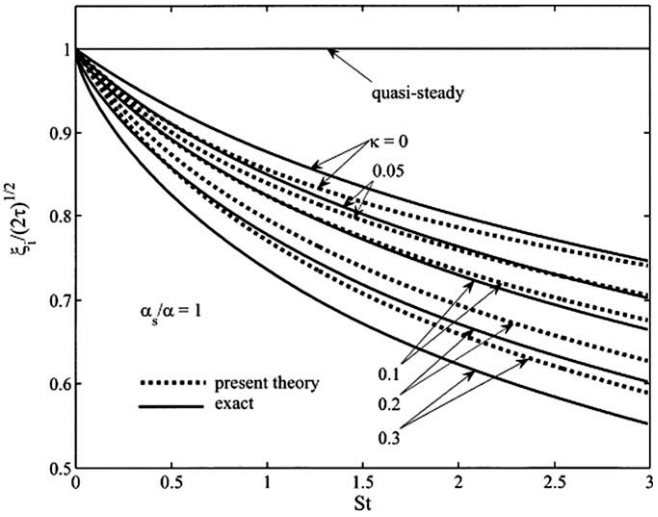

Fig. 3. Comparison with Neumann's planar solution, $\alpha_s/\alpha = 1$.

3.1.2. Test case 2: spherical probe

In this test case the interface solution is compared with the numerical solution to the freezing of tissue [16]. This solution takes into account blood perfusion but neglects metabolic heat production. Setting $\gamma = 0$ in (35),(36),(38) and (39) gives

$$a_1^2 + \kappa n a_1 b_2 - \frac{2}{St}\left[\frac{a_1}{(\xi_i - 1)} + \frac{1}{(\xi_i - 1)^2}\right] = 0, \tag{49}$$

$$n a_1 + \kappa n^2 b_2 - \frac{1}{St}\frac{\alpha}{\alpha_s}\left[n^2(1 - b_2) + n + \frac{\beta\xi_i^2}{b_2}\right] = 0, \tag{50}$$

$$n = \frac{1}{[\xi_i(\infty) - 1]\kappa} + \beta\kappa[1 - \xi_i(\infty)]\xi_i^2(\infty) - 1. \tag{51}$$

$$\xi_i(\infty) = \frac{\sqrt{\beta} - 1}{2\sqrt{\beta}} + \frac{1}{2\sqrt{\beta}}\left\{(1 - \sqrt{\beta})^2 + 4\sqrt{\beta}\left[1 + \frac{1}{\kappa}\right]\right\}^{\frac{1}{2}}. \tag{52}$$

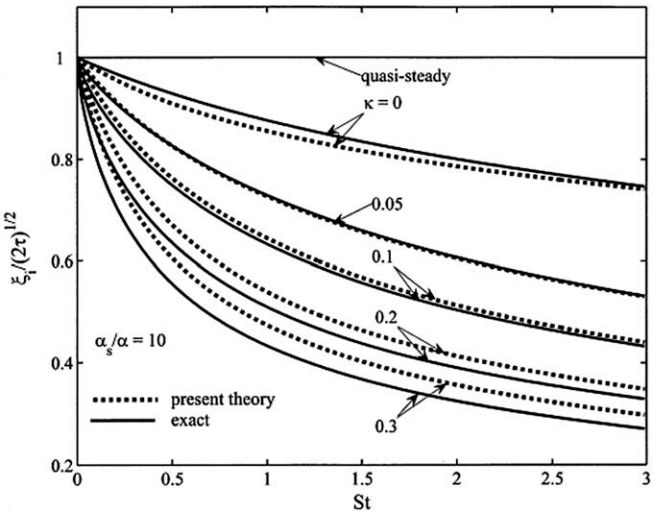

Fig. 4. Comparison with Neumann's planar solution, $\alpha_s/\alpha = 10$.

The numerical solution of [16] is based on a typical cryoprobe application of $\alpha_s/\alpha = 7$, $\beta = 0.336$, $\kappa = 1/7$ and $St = 0.517$. Substituting into (51) and (52) gives $\xi_i(\infty) = 3.701$ and $n = 1.728$. Using MATLAB to solve (49) and (50) for a_1 and b_2 as functions of ξ_i, substituting into (40) and integrating numerically gives $\xi_i(\tau)$. Fig. 5 compares the result of the present theory with the quasi-steady solution and the numerical solution to the governing Eqs. (1) and (2) presented in [16]. Since quasi-steady solutions are valid for small Stefan numbers, it is not surprising that for this case of $St = 0.517$ both quasi-steady and present theory give good results. Both approximate solutions converge to the exact steady state interface location.

3.2. Parametric studies

In general, tissue temperature and interface location are governed by five parameters: α_s/α, β, γ, κ and the Stefan number St. However, it is instructive to examine the relationship between St and κ. From their definitions in (3) and (11) we obtain

$$\kappa = \frac{k}{k_s}\frac{c_s(T_{a0} - T_f)}{\mathscr{L}}\frac{1}{St} \tag{53}$$

Except for T_{a0}, all quantities in the coefficient of St in (53) are tissue properties. However, since the variation in blood supply temperature T_{a0} is relatively small, the effect of κ will not be examined as an independent parameter.

Figs. 6–10 illustrate the effect of blood perfusion β, metabolic heat γ, Stefan number St and diffusivity ratio α_s/α on the interface motion associated with a planar probe. Selected values for these parameters are based on typical applications of cryoprobes. These results show that quasi-steady solutions predict faster interface motion than present theory. It should be recalled that quasi-steady solutions always overpredict the interface location. These results also show that increasing blood perfusion and/or metabolic heat production slows down interface motion and hastens the steady state condition. This is a consequence of adding more energy to the interface when these parameters are increased. Comparing Fig. 6 with Fig. 7 and Fig. 8 with Fig. 9 illustrates the slowing down of the interface motion as γ is increased from 0.05 to 0.1. On the other hand, increasing the Stefan number has the opposite effect on interface motion, as indicated by comparing Fig. 6 with Fig. 8 and Fig. 7 with Fig. 9. This follows from the fact that an increase in Stefan number corresponds to a decrease in latent heat of fusion leading to a faster moving

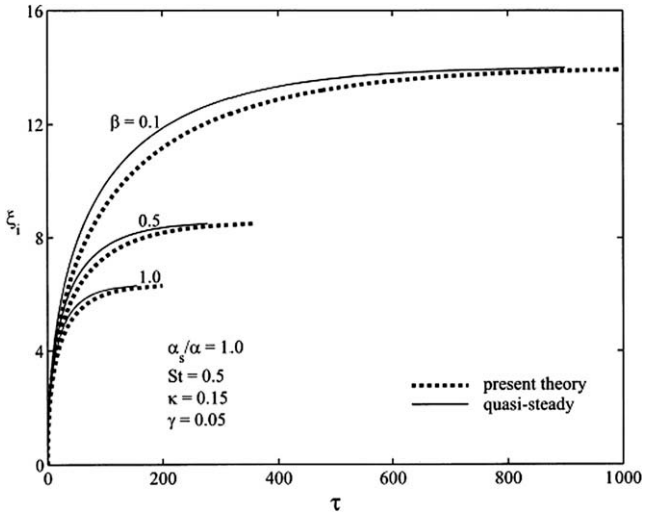

Fig. 6. Planar probe interface position, $\alpha_s/\alpha = 1$, $\gamma = 0.05$, $\kappa = 0.15$, $St = 0.5$.

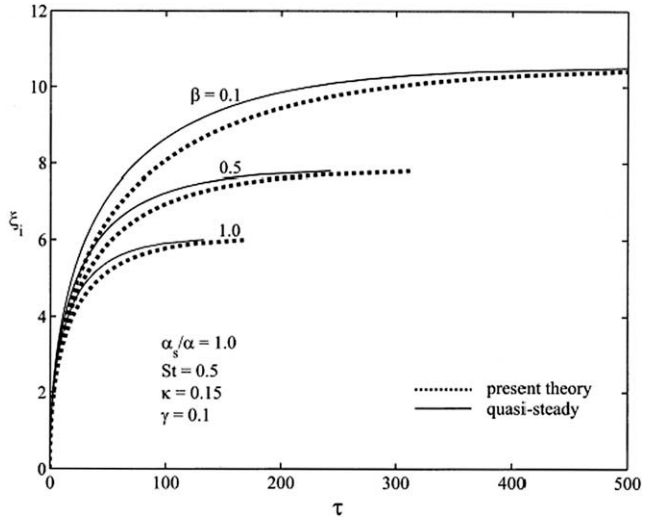

Fig. 7. Planar probe interface position, $\alpha_s/\alpha = 1$, $\gamma = 0.1$, $\kappa = 0.15$, $St = 0.5$.

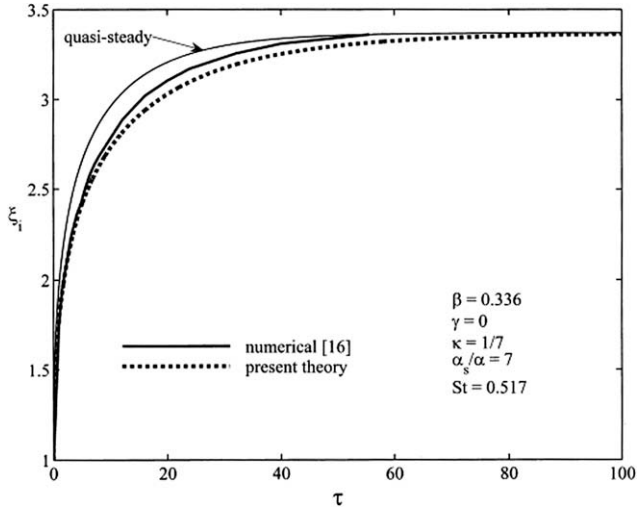

Fig. 5. Comparison with numerical solution of spherical probe.

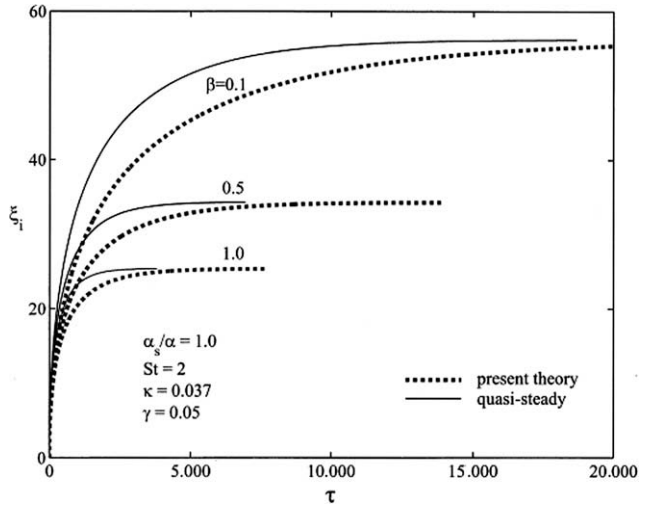

Fig. 8. Planar probe interface position, $\alpha_s/\alpha = 1$, $\gamma = 0.05$, $\kappa = 0.037$, $St = 2$.

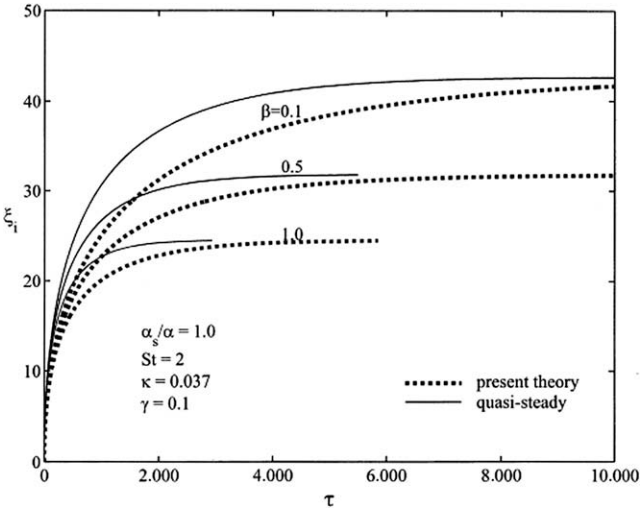

Fig. 9. Planar probe interface position, $\alpha_s/\alpha = 1$, $\gamma = 0.1$, $\kappa = 0.037$, $St = 2$.

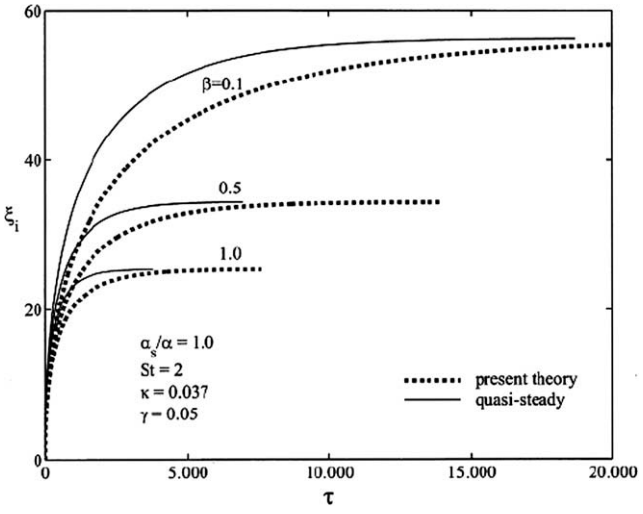

Fig. 10. Planar probe interface position, $\alpha_s/\alpha = 10$, $\gamma = 0.05$, $\kappa = 0.037$, $St = 2$.

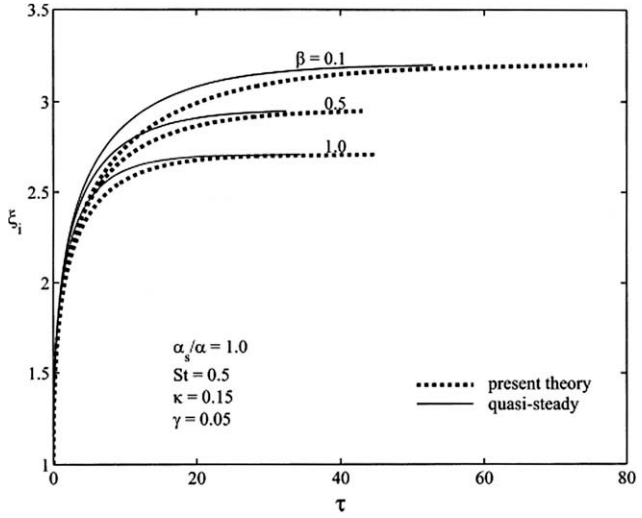

Fig. 11. Spherical probe interface position, $\alpha_s/\alpha = 1$, $\gamma = 0.05$, $\kappa = 0.15$, $St = 0.5$.

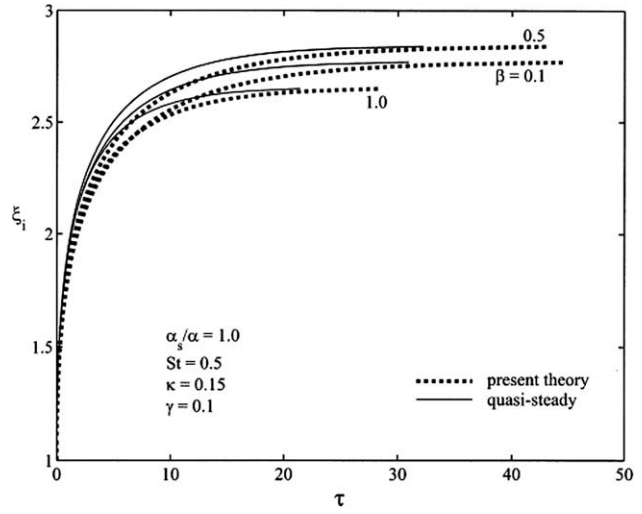

Fig. 12. Spherical probe interface position, $\alpha_s/\alpha = 1$, $\gamma = 0.1$, $\kappa = 0.15$, $St = 0.5$.

interface. The effect of thermal diffusivity ratio α_s/α on interface location is determined by comparing Fig. 8 with Fig. 10. Increasing α_s/α by a factor of 10 results in a small decrease in interface location. The decrease ranges from 0.002% for $\beta = 1.0$ and $\tau = 15{,}000$ to 7% for $\beta = 0.1$ and $\tau = 5{,}000$. Examination of Neumann's problem as well as all quasi-steady solutions shows that increasing α_s/α results in a decrease in interface location.

Parametric studies of the spherical probe is shown in Figs. 11–15. The effect of β, γ, St and α_s/α on interface location is qualitatively similar to that of the planar probe. Nevertheless, comparing the two geometries reveals significant differences for the same values of the governing parameters. Compared to the planar probe, steady state interface location is smaller and is reached faster for the spherical probe. However, interface speed is slower for the spherical probe. The blood perfusion parameter and Stefan number have a more pronounced effect on the planar probe than the spherical probe.

It should be noted that the special case of $\beta = \gamma = 0$ corresponds to Neumann's problem where a steady state does not exist. The trends in Figs. 6–15 are consistent with this limiting case.

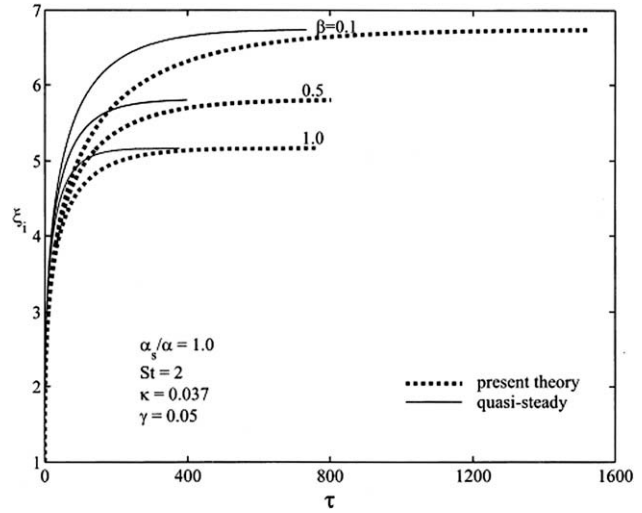

Fig. 13. Spherical probe interface position, $\alpha_s/\alpha = 1$, $\gamma = 0.05$, $\kappa = 0.037$, $St = 2$.

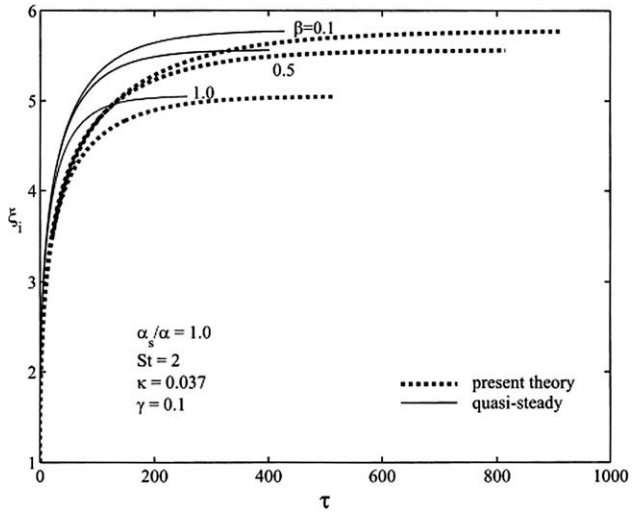

Fig. 14. Spherical probe interface position, $\alpha_s/\alpha = 1$, $\gamma = 0.1$, $\kappa = 0.037$, $St = 2$.

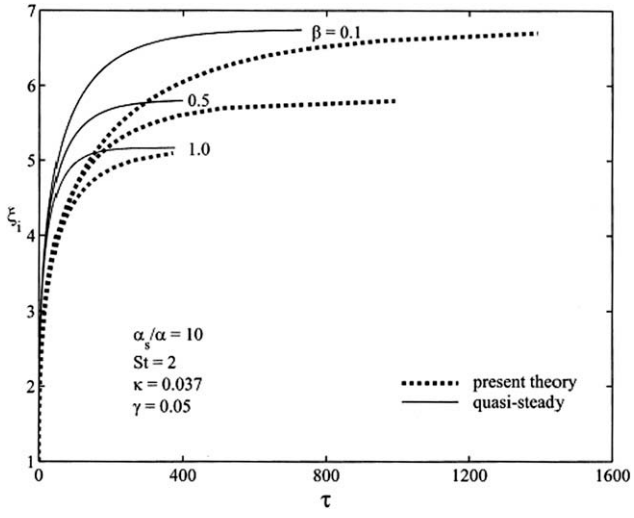

Fig. 15. Spherical probe interface position, $\alpha_s/\alpha = 10$, $\gamma = 0.05$, $\kappa = 0.037$, $St = 2$.

4. Conclusions

1. The present theory provides approximate analytic solutions to tissue freezing over planar and spherical probes. The solutions account for blood perfusion and metabolic heat production.
2. Unlike quasi-steady solutions, the present theory accounts for the Stefan number and thermal diffusivity ratio.
3. The solution to the temperature distribution in the frozen and unfrozen tissue satisfies all boundary conditions as well as the two heat equations at the interface.
4. The interface solution converges to the exact steady state interface condition.
5. The accuracy of the present theory is verified by comparison with Neumann's exact solution and a numerical solution to tissue freezing around a spherical probe.
6. The thermal diffusivity ratio α_s/α has a small effect on interface location. An increase in α_s/α by a factor of 10 results in an increase in interface location of less than 7%.
7. The effect of β, γ, St and α_s/α on interface location is qualitatively similar for both planar and spherical probes. However, blood perfusion and Stefan number have a more pronounced effect on the planar than the spherical probe.

References

[1] D.A. Tarzia et al., MAT-Serie A 2 (2000) 1–299.
[2] H.S. Carslaw, J.C. Jaeger, Conduction of Heat in Solids, Oxford at the Clarendon Press, 1959. pp. 283–296.
[3] Y. Rabin, A. Shitzer, Combined solutions of the inverse-Stefan problem for successive freezing/thawing in non-ideal biological tissues, J. Biomech. Eng. 119 (1997) 146–152.
[4] Y. Rabin, A. Shitzer, Exact solution to the one-dimensional inverse-Stefan problem in cryosurgical probe, J. Heat Transfer 117 (1995) 425–431.
[5] B. Rubinsky, A. Shitzer, Analysis of Stefan-like problem in a biological tissue around cryosurgical probe, J. Heat Transfer 98 (1976) 514–519.
[6] Z.S. Deng, J. Liu, Modeling multidimensional freezing problems during cryosurgery by dual reciprocity boundary element method, Eng. Anal. Bound. Elem. 28 (2004) 97–108.
[7] Y.T. Zhang, J. Liu, Numerical study on three-region thawing problem during cryosurgical re-warming, Med. Eng. Phy. 24 (2002) 265–277.
[8] Y. Rabin, A. Shitzer, Numerical solution of the multi-dimensional freezing problem during cryosurgery, J. Biomech. Eng. 120 (1998) 32–37.
[9] J.C. Rewcastle, G.A. Sandison, K. Muldrew, J.C. Saliken, B.J. Donnelly, A model for the time dependent three-dimensional thermal distribution within iceballs surrounding multiple cryoprobes, Med. Phys. 28 (2001) 1125–1137.
[10] R.I. Andrushkiw, Mathematical modeling of freezing front propagation in biological tissue, Math. Comput. Model. 13 (1990) 1–9.
[11] A. Weill, A. Shitzer, P. Bar-Yoseph, Finite element analysis of the temperature field around two adjacent cryoprobes, J. Biomech. Eng. 115 (1993) 374–379.
[12] J. Zhang, J.T.C. Hua, E.T. Chen, Experimental measurement and theoretical analysis of the freezing–thawing processes around a probe, Cryo Lett. 21 (2000) 245–254.
[13] A.J. Fic, Nowak, R. Bialecki, Heat transfer analysis of the continuous casting process by the front tracking BEM, Eng. Anal. Bound. Elem. 24 (2000) 215–223.
[14] I. Nowak, A.J. Nowak, L.C. Wrobel, Identification of phase change fronts by Bezier spines and NEM, Int. J. Therm. Sci. 41 (2002) 492–499.
[15] H.H. Pennes, Analysis of tissue and arterial blood temperatures in the resting forearm, J. Appl. Phys. 1 (1948) 93–122.
[16] G.J. Trezek, Thermal analysis for cryosurgery, in: A. Shitzer, R.C. Eberhart (Eds.), Heat Transfer in Medicine and Biology, vol. 2, Plenum Press, New York, 1985, pp. 239–258.
[17] S. Chakraborty, P. Dutta, Analytical solutions for heat transfer during cyclic melting and freezing of a phase change material used in electronic or electrical packaging, J. Electron. Packaging 125 (2003) 126–133.
[18] C.K. Hsieh, M. Leung, Phase change in a cylinder and cylindrical shell heated with an axisymmetric front moving in the axial direction, J. Heat Transfer 123 (2001) 476–485.
[19] T.J. Lu, Thermal management of high power electronics with phase change cooling, Int. J. Heat Mass Transfer 43 (2000) 2245–2256.
[20] W.J. Song, L.M. Jiji, Peripheral tissue freezing in cryosurgery, Cryosurgery 25 (1988) 153–163.
[21] S. Lin, J. Zheng, An improved quasi-steady analysis for solving freezing problems in a plate, a cylinder and a sphere, J. Heat Transfer 125 (2003) 1123–1128.